Liu *et al. Journal of Hematology & Oncology* (2024) 17:122
https://doi.org/10.1186/s13045-024-01648-0

Journal of Hematology & Oncology

RESEARCH Open Access

Engineering a controllable and reversible switch for CAR-based cellular immunotherapies via a genetic code expansion system

Yue Liu[1,2†], Lingna An[1,2†], Xiaoqi Wang[1,2†], Yueyu Dai[1,2], Cheng Zhang[1,2*], Qin Wen[1,2*] and Xi Zhang[1,2,3*]

Abstract

Background As one of the most promising adoptive cell therapies, CAR-T cell therapy has achieved notable clinical effects in patients with hematological tumors. However, several treatment-related obstacles remain in CAR-T therapy, such as cytokine release syndrome, neurotoxicity, and high-frequency recurrence, which severely limit the long-term effects and can potentially be fatal. Therefore, strategies to increase the controllability and safety of CAR-T therapy are urgently needed.

Methods In this study, we engineered a genetic code expansion-based therapeutic system to achieve rapid CAR protein expression and regulation in response to cognate unnatural amino acids at the translational level. When the unnatural amino acid *N-ε-((tert-butoxy) carbonyl)-l-lysine* (BOCK) is absent, the CAR protein cannot be completely translated, and CAR-T is "closed". When BOCK is present, complete translation of the CAR protein is induced, and CAR-T is "open". Therefore, we investigated whether the BOCK-induced device can control CAR protein expression and regulate CAR-T cell function using a series of in vitro and in vivo experiments.

Results First, we verified that the BOCK-induced genetic code expansion system enables the regulation of protein expression as a controllable switch. We subsequently demonstrated that when the system was combined with CAR-T cells, BOCK could effectively and precisely control CAR protein expression and induce CAR signaling activation. When incubated with tumor cells, BOCK regulated CAR-T cells cytotoxicity in a dose-dependent manner. Our results revealed that the presence of BOCK enables the activation of CAR-T cells with strong anti-tumor cytotoxicity in a NOG mouse model. Furthermore, we verified that the BOCK-induced CAR device provided NK cells with controllable anti-tumor activity, which confirmed the universality of this device.

†Yue Liu, Lingna An and Xiaoqi Wang contributed equally to this work.

*Correspondence:
Cheng Zhang
chzhang2014@tmmu.edu.cn
Qin Wen
qiqi105@sina.com
Xi Zhang
zhangxxi@sina.com; zhangxi@tmmu.edu.cn

Full list of author information is available at the end of the article

Conclusions Our study systematically demonstrated that the BOCK-induced genetic code expansion system effectively and precisely regulates CAR protein expression and controls CAR-T cell anti-tumor effects in vitro and in vivo. We conclude that this controllable and reversible switch has the potential for more effective, secure, and clinically available CAR-based cellular immunotherapies.

Keywords CAR-based cellular immunotherapies, Controllable and reversible, Switch, Genetic code expansion system, BOCK

Background

Chimeric antigen receptor T (CAR-T) cell immunotherapy based on engineered T cells with recombinant antigen-specific CAR molecules has become a powerful and promising adoptive cell therapy for malignant tumors in the last decade [1, 2]. Specifically, for patients with refractory or relapsed B acute lymphoblastic leukemia (B-ALL), CD19 CAR-T cell therapy has shown significant and durable anti-tumor clinical efficacy [3, 4]. On the basis of these dramatic clinical successes, a series of CAR-T products with substantial clinical value have been approved in the United States and China in recent years [5–8]. Despite the prominent clinical efficacy of CAR-T therapy in B-ALL, several challenges remain, including limited effectiveness against solid tumors, cytokine release syndrome (CRS), immune effector cell-associated neurotoxicity syndrome (ICANS), and a high recurrence rate caused by poor CAR-T cells persistence after refusion [9–11]. For superior CAR-T cells with better clinical manifestations and efficacy, several optimization strategies have been developed, including exploring new and suitable tumor targets, designing CAR structures for flexible T cell activation, inhibiting checkpoints to improve tumor killing, and regulating metabolism and differentiation for longer persistence [12–16].

A critical balance exists between high efficiency tumor elimination and CRS induced by vigorous activation of CAR-T cells [10, 17]. Severe and drastic CRS might induce excessive inflammation and capillary leakage, leading to organ damage, brain swelling, and ultimate death [17]. In a large multi-center observational cohort of large B cell lymphoma patients treated with a CAR-T cell product (axicabtagene ciloleucel), over 90% of patients developed CRS [18, 19]. Moreover, excessive activation of CAR-T cells leads to early exhaustion and disability [20, 21]. Therefore, balancing the efficiency and side-effects of CAR-T therapy is a major challenge [22]. Several logic-gated and switch-receptor strategies have been explored to flexibly and spatially control CAR-T cell function [23]. To prevent side-effects, researchers have designed suicide devices for CAR-T cells by fusing Caspase 9 together with a modified human FK-binding protein [24, 25]. This device can cause rapid death and eliminate more than 90% of CAR-T cells [24]. Dasatinib, a typical tyrosine kinase inhibitor, prevents the downstream signaling of the CAR domain and inhibits CAR-T cell activation [26]. Dasatinib reduces the CRS ratio in a lymphoma mouse model. These function-off devices and measures could efficiently prevent severe toxicity to ensure CAR-T safety, but they also limit long-term CAR-T function. Surprisingly, synthetic and genetic biology have provided new solutions. Reversible devices and approaches for controlling CAR-T function have been designed and developed [27–32]. A resveratrol-responsive trans-activator and trans-repressor were used to develop a controllable transgene expression device [33]. This system was optimized to control CAR protein expression and CAR-T cell anti-tumor function using a resveratrol-titratable mechanism, with the potential for increasing CAR-T therapy safety [33]. An inhibitory protease-regulatory system controlled by an FDA-approved small molecule was combined with CAR-T cells [34]. This platform enables remote tuning of CAR activity and shows no leaky activity and outperforms constitutive CAR-T cells [34]. These devices endow CAR-T therapy with flexibility and promote the clinical efficacy and safety of this treatment.

Here, to improve the safety and controllability, we designed and manipulated a controllable and reversible switch for CAR-T cell therapy by introducing a genetic code expansion system. According to the genetic central dogma, tRNA orthogonally recognizes codons and transfers amino acids into the polypeptides for protein translation. In the absence of an orthogonal tRNA, three STOP codons (TAA, TAG, and TGA) cannot be recognized, and their presence indicates the termination of the translation process. Recently, orthogonal tRNA/aminoacyl-tRNA synthetase (aaRS) pairs recognizing STOP codons have been discovered in some archaea and bacteria [35–37]. These tRNA/aaRS pairs were subsequently designed and remolded for use as controllable gene manipulation platforms [38–42]. This system enables tight control of complete mRNA translation by overcoming termination signaling in the STOP codon and incorporating unnatural amino acids (UAAs) into the target protein [43]. In this study, we developed an UAA triggered CAR-T cell therapy platform composed of the aaRS-tRNACUA pair and a CAR gene carrying an ectopic STOP codon. We demonstrated that this system can effectively regulate CAR protein expression using an UAA-titratable mechanism. The anti-tumor effect was also flexibly controlled by the addition and withdrawal of UAA. The response of this system can be detected after 4 h of triggering and without

any leaky activity. Unexpectedly, we also found that the system induced CAR-T cells with decreased exhaustion and an increased ratio of memory subsets for longer persistence. In a B-ALL mouse model, T cells loaded with this reversible CAR system efficiently eliminated tumors in the presence of UAA. Moreover, we demonstrated that the reversible device provides NK cells with controllable anti-tumor activity. Thus, our study manipulated a reversible CAR device via a genetic code expansion system that enables flexible control of CAR activity and antitumor efficacy, providing a new approach and potential for increasing the safety and efficacy of CAR-based cellular immunotherapies.

Methods

Plasmid construction and preparation

The coding sequences of pyrrolysyl-aaRS (PylRS) and orthogonal tRNA from *Methanosarcina mazei* were obtained from Addgene Plasmid (#174526 and #174890) [44, 45]. EF1a was designed as the promoter of PylRS. U6 was the promoter of tRNA. The mCherry and EGFP genes were engineered as a reporter. A termination codon, TAG, was incorporated into the 150th amino acid of EGFP, as shown in Fig. 1A. The three cassettes were subsequently cloned and inserted into a vector backbone containing the PiggyBac transposon. The CD19 CAR sequence was obtained from Kymirah [46]. TAG was individually incorporated into the front, middle, and rear sites of CAR sequence, as shown in Fig. 1D. The CARs were constructed via Gibson assembly to replace the mCherry-EGFP cassette. Moreover, eight tandem repeats of the tRNA cassette were introduced to improve

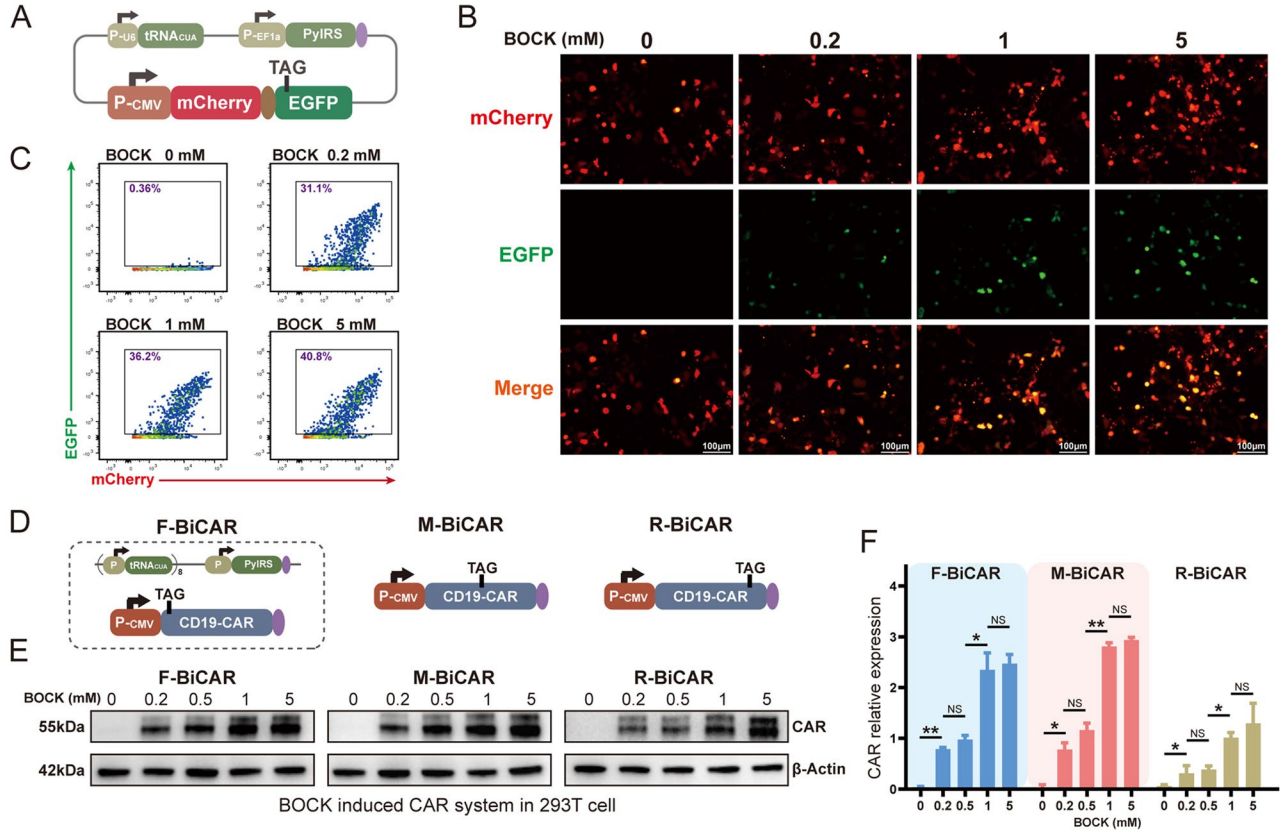

Fig. 1 Design and characterization of the reversible CAR protein expression device induced by the genetic code expansion system. **A** Schematic representation of the genetic code expansion system, including $tRNA_{CUA}$, the orthogonal aminoacyl-tRNA synthetase (aaRS), and a dual fluorescent protein expression cassette. **B&C** EGFP protein expression in 293T cells incubated with different concentrations of BOCK, as detected by flow cytometry and fluorescence microscopy. **D** Schematic representation of the BiCAR expression system, in which TAG was inserted into the CAR coding region, individually located between the initiation codon and the CD19 ScFv (the front BiCAR, F-BiCAR), between the CD19 ScFv and the CD8 spacer (the middle BiCAR, M-BiCAR), and between the 4-1BB costimulatory domain and the CD3 zeta domain (the rear BiCAR, R-BiCAR). **E&F** Western blot analysis showed the expression level of the CAR protein in the three BiCAR systems induced by BOCK addition. The data are reported as the means ± SDs ($n = 3$). *$p < 0.05$, **$p < 0.01$, ***$p < 0.001$, not significant (ns) by t tests

the translation efficacy. The vector containing the PiggyBac transposase was purchased from Genechem Co., Ltd (Shanghai, China). The above sequences are listed in Table S1.

Cell lines and cell culture

Embryonic kidney 293T cells were cultured in DMEM (BI, Israel) supplemented with 10% FBS (BI, Israel). Jurkat T cells and Nalm6-luciferase (Nalm6-Luc) cells were cultured in RPMI-1640 (BI, Israel) supplemented with 10% FBS (BI, Israel). NK92 cells were cultured in MEMα supplemented with 0.2 mM inositol, 0.1 mM β-mercaptoethanol, 0.02 mM folic acid, 12.5% horse serum, and 12.5% FBS (Pricella Life Science & Technology, China) with 200 U of IL-2 (MCE, USA). All cell lines were maintained at 37 °C in a cell culture incubator (Thermo Fisher, USA) with a humidified 5% CO_2 atmosphere.

Plasmid electroporation and sorting

For sufficient transfection efficiency, electroporation was performed via an electroporator (Celetrix LLC, USA). First, 2 μg of plasmid mixture was mixed immediately before electroporation. A total of 2.5×10^6 cells were collected and resuspended in 20 μL of buffer (half buffer A and half buffer B). Then, the plasmid mixture was added to the buffer, and the mixture was incubated for 10 min at room temperature. The mixture was transferred to an electric tube and electroporated at 420 V, 20 ms for 293T cells, 480 V, 20 ms for $CD3^+$ T cells, 520 V, 20 ms for Jurkat T cells, and 530 V, 20 ms for NK92 cells. Following electroporation, the cells were transferred into complete medium. Then, cells were supplemented with 2 mM BOCK. After 48 h, CAR-positive cells were obtained by sorting with a Moflo XDP (Beckman Coulter, USA).

Chemicals

The UAA, *N-ε-((tert-butoxy) carbonyl)-l-lysine* (BOCK) (CAS: 2418-95-3) (Fig. S1A) was purchased from Haohong Biological Medicine Technology Co., Ltd (Shanghai, China). For in vitro cell culture, BOCK was prepared in 200 mM stock solutions in ddH_2O at 65 ℃ to accelerate dissolution and stored at -80 ℃. The stock solution was diluted to the final working concentrations via culture medium immediately before addition. For the xenograft mouse tumor model assay, BOCK was prepared in PBS and intraperitoneally injected (20 mg per mouse, every two days). Dasatinib (MCE, USA) was prepared in 10 mM stock solutions and stored at -80 ℃.

Primary CD3+ T cell isolation, activation and proliferation

Peripheral blood mononuclear cells (PBMCs) were obtained from healthy donors and patients according to ethical, moral, and safety requirements. Primary human $CD3^+$ T cells were isolated from PBMCs using CD3 MicroBeads (Miltenyi Biotec, Germany) and activated with anti-CD3/CD28 beads (Thermo Fisher, USA) (1:1 cell/bead ratio) in X-VIVO 15 (Lonza, Switzerland) medium supplemented with 200 U of IL-2 (MCE, USA). The medium was renewed every two days, and the cells were maintained at 1×10^6 cells/mL for proliferation and subsequent experiments.

Flow cytometric analysis of cell surface markers

For cell surface marker detection, 10^6 cells were centrifuged at 300 × g for 5 min and resuspended in 100 μL of PBS supplemented with 2% FBS. The flow cytometric antibodies for surface markers were added into the staining buffer, including APC-anti-CD69 (BioLegend, USA), APC/Cy7-anti-CD25 (BD Pharmingen, USA), PE/Cy7-anti-CD8 (BioLegend), PE-anti-CD4 (BD Pharmingen), APC-anti-CD62L (BD Pharmingen), PE-anti-CD45RO (BD Pharmingen), PE-anti-PD-1 (BioLegend), PE-anti-CD56 (BioLegend) PE/Cy7-anti-NKG2D (BioLegend), FITC-Streptavidin (BioLegend), PE-Streptavidin (BioLegend), CD19-ADA-biotin (ACRO Biosystems), PE/Cy7-anti-CTLA-4 (BioLegend), and FITC-anti-$(G4S)_n$ (Hycells, China). The samples were incubated at 4 ℃ for 30 min. The cells were subsequently washed twice and resuspended in 0.5 mL of PBS for flow cytometric analysis (Beckman Dickinson LSRFortessa, USA).

Flow cytometric analysis of intracellular cytokines

For intracellular cytokines staining, effector cells were first incubated with the CD19 antigen protein (ACRO Biosystems) or with Nalm6-Luc cells (ratio of 1:1) in the presence or absence of BOCK. The medium contained 1 × Brefeldin A Solution (BioLegend). After incubation for 6 h or overnight, intracellular cytokine staining was performed using a Cyto-Fast™ Fix/Perm Buffer Set (BioLegend) according to the manufacturer's instructions. Briefly, 1×10^6 cells were centrifuged at 300 × g for 5 min, resuspended in 100 μL of Cyto-Fast™ Fix/Perm Buffer and mixed gently. The mixture was incubated for 20 min at room temperature. Then, 1 mL of 1 × Cyto-Fast™ Perm Wash solution was added and the mixture was centrifuged at 350 × g for 5 min. The cells were stained with intracellular antibodies at room temperature in the dark, including APC-anti-TNF-α (BioLegend), PE-anti-GZMB (BioLegend), APC/Cy7 anti-IFN-γ (BioLegend), APC-anti-IL-2 (BioLegend), and PE-anti-GM-CSF (BioLegend). The cells were washed with 1 mL of 1 × Cyto-Fast™ Perm Wash solution and centrifuged at 350 × g for

5 min. Finally, the cells were resuspended in 400 μL of Cell Staining Buffer for flow cytometric analysis. For the degranulation assay, Nalm6-Luc cells (ratio of 1:1), APC/Cy7-anti-CD107a (BioLegend), and Brefeldin A were added to the effector cells. After 4 h, the samples were collected for flow cytometric analysis.

Coculture cytotoxicity assay

The cytotoxicity of the effector cells was evaluated via a luciferase-based assay. A total of 10^4 Nalm6-Luc cells in 100 μL of culture medium were seeded into the wells of a white 96-well plate (Beyotime, China). Effector cells were coincubated with Nalm6-Luc cells at the indicated ratios and for the indicated times. Triplicate wells were plated for each group, and the viability of Nalm6 cells was detected via a Bio-Lite Luciferase Assay System (Vazyme, China). The cytotoxicity was quantified as follows: lysis (%) = (no effector cell groups) − (effector cell and tumor cell coculture groups) / (no effector cell groups) × 100%.

Western blot analysis

For protein detection, target cells were lysed in NP-40 lysis buffer (5×10^5 cells with 50 μL) supplemented with protease and phosphatase inhibitor cocktail (Beyotime) for approximately 30 min. The cell lysates were collected via centrifugation at 13,000 rpm at 4 °C for approximately 10 min. Then, the protein from each sample was boiled with loading buffer for 5 minutes. The isolated protein was subjected to SDS-PAGE on 4 −20% polyacrylamide gels (ACE Biotechnology, China), and electroblotted onto nitrocellulose filter membranes (Millipore, USA). The membrane was blocked with 5% non-fat milk in TBST at room temperature for approximately 1 h and then incubated with the relevant primary antibody and secondary antibody. The primary antibodies were diluted in Primary Antibody Dilution Buffer (Beyotime), including anti-HA tag antibody (1:3000, CST), anti-β-actin antibody (1:5000, Beyotime), anti-PLC antibody (1:3000, Abcam), anti-p-PLC antibody (Tyr783, 1:3000, CST), anti-SLP76 antibody (1:3000, Solarbio), anti-p-SLP76 antibody (Ser376, 1:3000, CST), anti-ZAP70 antibody (1:3000, Beyotime), anti-p-ZAP70 antibody (Tyr493/526, 1:3000, CST), anti-LCK antibody (1:3000, Beyotime), anti-p-LCK antibody (Tyr505, 1:3000, CST), anti-LAT antibody (1:3000, Abcam), anti-p-LAT antibody (Tyr220, 1:3000, CST), anti-AKT antibody (1:3000, Beyotime), anti-p-AKT antibody (T308, 1:3000, Abcam), anti-mTOR antibody (1:3000, Beyotime), anti-p-mTOR antibody (S2448, 1:3000, Abcam), anti-RPS6 antibody (1:3000, Beyotime), and anti-p-RPS6 antibody (Ser235/236, 1:3000, Beyotime). The secondary antibodies were diluted in TBST, including HRP-labeled goat anti-rabbit and HRP-labeled goat anti-mouse antibodies (Beyotime). After the two-step incubation and washing, the membranes were incubated with West Femto Maximum Sensitivity Substrate (Thermo Fisher) and visualized with a ChemiDoc XRS$^+$ System (Bio-Rad, USA).

qRT-PCR analysis

Total RNA obtained from target cells was extracted via the RNAiso Plus reagent (TaKaRa, Japan) following the manufacturer's instructions. Then, 0.5 μg of total RNA was subjected to reverse transcription with One-Step gDNA Removal and cDNA Synthesis SuperMix (TransGen Biotech, China). Quantitative real-time PCR (qRT-PCR) was performed using SYBR® Premix Ex Taq™ II (TaKaRa, Japan) via the CFX Connect RealTime PCR Detection System (Bio-Rad, USA). The expression levels of target genes were normalized to that of GAPDH (internal control). The primer sequences for target genes are shown in Table S2.

Biosafety assay of BOCK in mice

To determine the biosafety of BOCK in mice during long-term uptake, 8- to 10-week-old female C57BL/6 mice were intraperitoneally injected with BOCK (20 mg per mouse) or PBS every two days (six mice in each group). The weight was continuously monitored every five days. Thirty days after injection, blood samples were collected for routine blood examination, including white blood cell (WBC), neutrophilic granulocyte (NEUT), lymphocyte (LYM), monocyte (MXD), hemoglobin (HGB), red blood cell (RBC), mean corpuscular hemoglobin (MCH), and platelet (PLT) analyses.

Xenograft mouse tumor model assay

To analyze the induction efficacy of BOCK in vivo, 6- to 8-week-old immunocompromised female NOD.Cg-*Prkdc scid* mice (NOG mice) from Beijing Vitalstar Biotechnology were intraperitoneally injected with 2×10^7 BiCAR-T cells in 200 μL of PBS. Four hours after BiCAR-T cells implantation, the mice were administrated BOCK at doses ranging from 0 to 20 mg per mouse. Twenty hours after BOCK injection, the mice were sacrificed by cervical dislocation, and peritoneal cells were collected, stained and detected via flow cytometry.

To evaluate of BiCAR-T cell function in vivo, a human leukemia model was created using 6- to 8-week-old female NOG mice. Briefly, 1.5×10^6 Nalm6-Luc cells in 150 μL of PBS were tail-intravenously. After 7 days, the mice were randomly assigned (four/five mice per group), and 1×10^6 conventional CAR-T cells or the indicated BiCAR-T cells were tail-intravenously injected with 100 μL of PBS. BiCAR-T cells were sorted before refusion for CAR positive cells in the presence of BOCK. BOCK was intraperitoneally injected every two days at a dose of 20 mg per mouse. Tumor burden progression was monitored and measured every 7 days following

the intraperitoneal injection of D-Luciferin potassium salt (150 mg/kg, Beyotime) using the BURKER In-Vivo XtremeII Platform. The mice were humanely euthanized when they showed signs of morbidity and/or hindlimb paralysis. To evaluate BiCAR-NK cell function in vivo, a human leukemia model was created using 6- to 8-week-old female NOG mice. Briefly, 1.5×10^6 Nalm6-Luc cells in 150 μL of PBS were tail-intravenously. After 7 days, the mice were randomly assigned (five mice per group), and 5×10^6 CAR-NK cells or the indicated BiCAR-NK cells were tail-intravenously injected with 200 μL of PBS on Day8, Day15, Day22, and Day29. BOCK was intraperitoneally injected every two days at a dose of 20 mg per mouse. The tumor burden monitoring was conducted in a manner similar to that noted for the BiCAR-T system.

Results

Design and manipulation of a reversible CAR switch via a genetic code expansion system

First, we constructed a genetic code expansion system based on the widely used aaRS-tRNACUA pair from *Methanosarcina mazei* and the UAA, *N-ε-((tert-butoxy) carbonyl)-l-lysine* (BOCK) (Fig. 1A, S1A) [44]. A dual fluorescent protein expression cassette (mCherry-EGFP) was engineered as a reporter. A PylRS-tRNACUA pair was inserted. The coding region of EGFP harbored a termination codon TAG. It can be recognized, bound, and translated by aaRS-tRNACUA pair and BOCK. When this system is transfected into cells, the mCherry protein is continuously produced, whereas EGFP protein expression could only be triggered by the smooth translation of TAG in the presence of BOCK. Otherwise, the translation stops at the TAG site in the absence of BOCK. Therefore, the mCherry-EGFP dual fluorescent protein can be used to determine and evaluate the function and efficacy of the genetic code expansion system induced by BOCK. In human embryonic kidney 293T (HEK293T) cells transfected with this system, the EGFP protein was rapidly produced upon the addition of BOCK, as shown by fluorescence microscopy (Fig. 1B). The EGFP protein was maintained at an extremely low level in the absence of BOCK, which suggests a high activation/inactivation ratio according to the flow cytometric analysis (Fig. 1C). Moreover, we found that the EGFP protein was quickly degraded after the withdrawal of BOCK from the culture medium, indicating complete and sensitive reversibility (Fig. S1B). Therefore, the BOCK induced genetic code expansion system can effectively and delicately control target protein expression as a reversible switching device.

Therefore, we next attempted to optimize CAR-T cell therapy by combining the genetic code expansion system as a reversible switch. The termination codon TAG was inserted into the CAR protein coding region, with translation theoretically occurring in the presence of PylRS-tRNACUA pairs and being induced by BOCK, resulting in what is termed as BOCK induced CAR (BiCAR) system. Three TAG stop codons were separately inserted: one individually located between the initiation codon and the CD19 scFv (the front BiCAR, F-BiCAR), one between the CD19 scFv and the CD8 spacer (the middle BiCAR, M-BiCAR), and one between the 4-1BB costimulatory domain and the CD3 zeta domain (the rear BiCAR, R-BiCAR) (Fig. 1D) (Table S1). These sites were chosen to prevent interference the function of the CAR. Western blot results revealed that all three BiCARs were effectively induced by BOCK addition in a concentration dependent manner (Fig. 1E). In addition, we found that F-BiCAR and M-BiCAR had similar translational efficiencies, both of which were greater than that of R-BiCAR (Fig. 1F). Thus, they were used for subsequent experiments. Collectively, our initial results in HEK293T cells demonstrated that BOCK can effectively activate the genetic code expansion system via the PylRS-tRNACUA pair and control CAR protein expression.

Characterization performance and function of reversible BiCAR-Jurkat T cells

As a cell line derived from acute T lymphocytic leukemia, Jurkat T (JT) cells have been widely used in studies on T cell signal transduction and cytotoxic functions. Therefore, we profiled the effects of the BiCAR system on JT cells induced by BOCK (Fig. 2A). To exclude any unanticipated impacts of BOCK on JT cells, we profiled the effects of BOCK by analyzing cell viability, and the results demonstrated that 5 mM BOCK had no obvious effect on JT cells (Fig. S1C). The F-BiCAR and M-BiCAR systems were transfected into JT cells to construct BiCAR-JT devices. The two BiCAR-JT cells exhibited efficient and dose-dependent BOCK induced CAR protein expression (Fig. 2B). Next, we investigated whether BOCK induced CAR expression regulates JT cell activation and function. In the presence of antigens, CAR can deliver this signal to the intracellular receptors and activate them. We found that the addition of BOCK increased the phosphorylation levels of CAR downstream signals, including p-LCK (Tyr505), p-ZAP70 (Tyr493/526), p-LAT (Tyr220), p-SLP76 (Ser376), and p-PLCγ1 (Tyr783) in a dose dependent manner (Fig. 2C upper). The Akt-mTOR signaling was subsequently phosphorylated to promote T cell function (Fig. 2C, lower). For further analysis of the anti-tumor cytotoxicity, BiCAR-JT cells were pretreated with BOCK at different concentrations and then cocultured with Nalm6-Luc cells at different effector/target ratios and incubation times. The luciferase activity detection results revealed that the cytotoxicity of BiCAR-JT cells to Nalm6-Luc cells was precisely and flexibly controlled by the BOCK dose (Fig. 2D). Specifically,

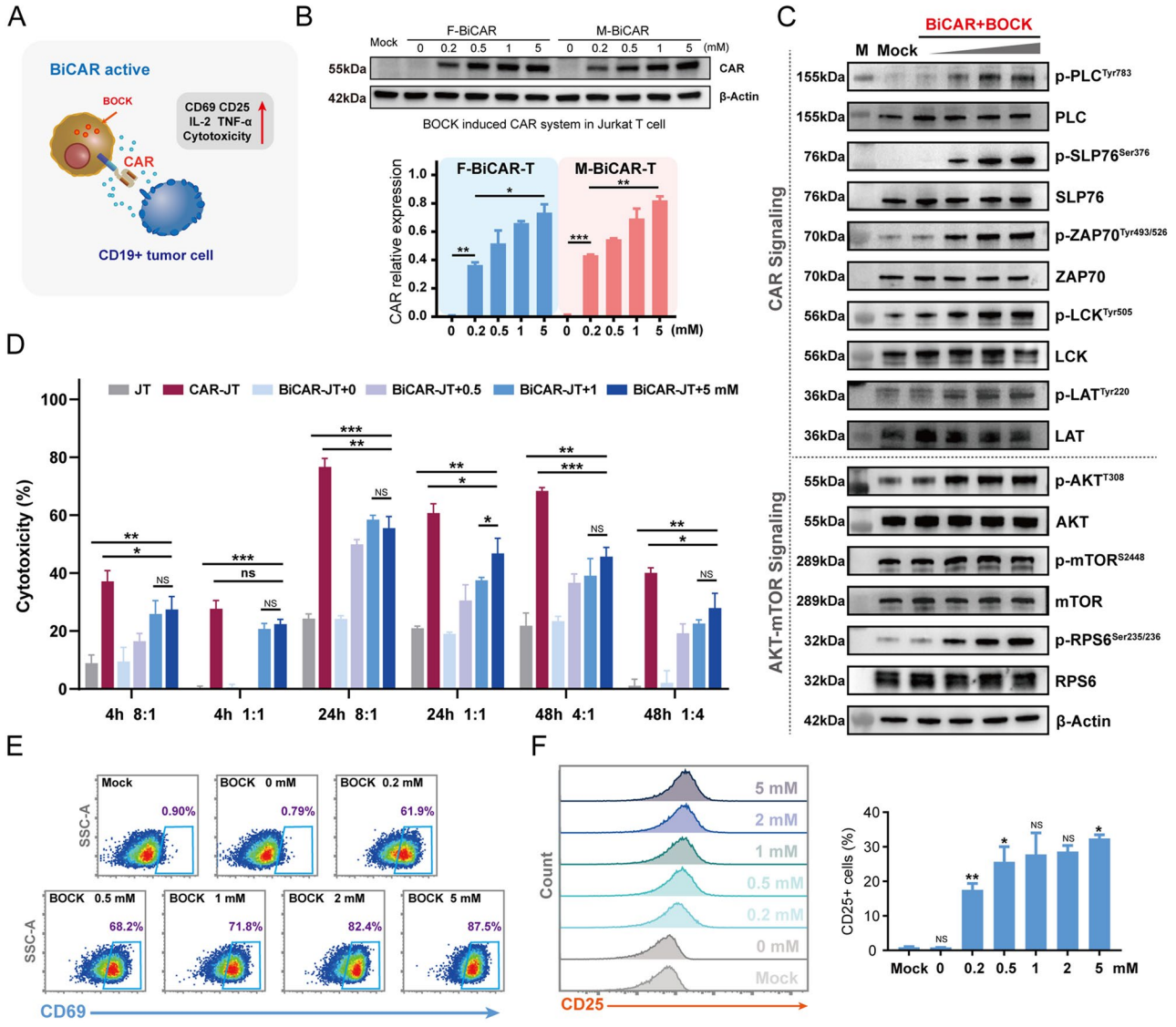

Fig. 2 Characterization and cytotoxicity of the reversible BiCAR-Jurkat T cells. **A** Scheme of the BiCAR device for Jurkat T cells. **B** Western blot analysis showed that BOCK efficiently induced CAR protein expression. The data are reported as the means ± SDs ($n = 3$). **C** Western blot analysis showed that BOCK induced CAR protein could increase the downstream phosphorylation events of CAR signaling (upper) and AKT-mTOR signaling (lower) in a dose dependent manner after stimulation with the antigen. **D** The cytotoxicity of BiCAR-JT cocultured with Nalm6-Luc cells and BOCK for 4, 24, 48 h at different effector/target (E/T) ratios. The data are reported as the means ± SDs ($n = 3$). **E** Flow cytometry showed that CD69 was activated by BiCAR-JT cells exposed to BOCK and antigens. **F** Flow cytometry showed that CD25 was activated by BiCAR-JT cells exposed to BOCK and antigens. The data are reported as the means ± SDs ($n = 3$). $^{*}p < 0.05$, $^{**}p < 0.01$, $^{***}p < 0.001$, not significant (ns) by t tests

BiCAR-JT cells treated with 1 mM and 5 mM BOCK showed similar cytotoxicity, both of which were greater than that of 0.5 mM, but slightly less than that of the positive control, conventional CAR-JT cells. Moreover, CD69 and CD25, two well-defined and general T cell surface early activation markers, were activated in the presence of BOCK and antigen stimulation, demonstrating that the CAR signaling strength was precisely regulated by BOCK (Fig. 2E and F). IL-2 and TNF-α, two important factors for effector T cell activation and function, were also triggered in a BOCK dose-dependent manner (Fig. S2A - S2C). In summary, these results demonstrated that the BOCK-induced genetic code expansion system could delicately regulate CAR protein expression, CAR signaling mediated activation, and cytotoxicity in JT cells.

Characterization performance and function of the reversible BiCAR system in primary T cells

We further developed a reversible BiCAR system in primary T cells. The BiCAR system was electro-transfected into primary $CD3^{+}$ T cells isolated and activated from PBMCs. The BiCAR system was closed, and the CAR

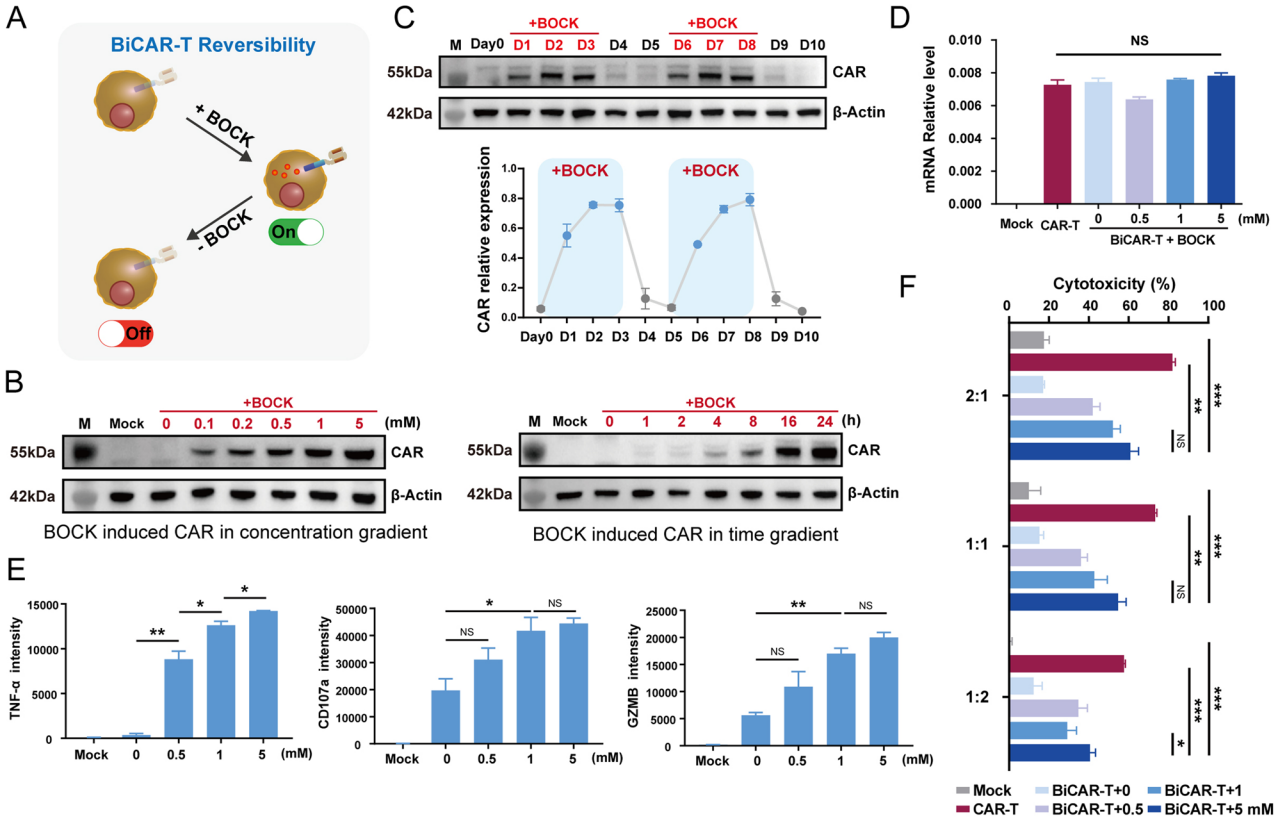

Fig. 3 Characterization and performance of the reversible BiCAR-T cells. **A** Scheme of the reversible BiCAR device in primary T cells. **B** Western blot assays showed that BOCK could induce the BiCAR system in a concentration and time dependent manner. **C** Western blot assays showed the reversibility of BiCAR device-mediated CAR expression in primary T cells. BOCK was added on Day1–3 and Day6–8, while it was withdrawn on Day4–5 and Day9–10. **D** qPCR assay revealed that the mRNA level of CAR in the BiCAR device was stable regardless of the presence of BOCK. **E** The release of cytokines including TNF-α and GZMB, and the CD107a degranulation of BiCAR-T cells with BOCK at different concentrations when they were cocultured with Nalm6 cells for 24 h. **F** The cytotoxicity of the BiCAR-primary T cells cocultured with Nalm6-Luc cells and BOCK for 48 h at E/T ratios (2:1, 1:1, and 1:2). The data are reported as the means ± SDs ($n = 3$). *$p < 0.05$, **$p < 0.01$, ***$p < 0.001$, not significant (ns) by t tests

protein could not be detected when BOCK was absent. After the addition of BOCK to the culture medium, the device was activated, and the CAR protein was detected (Fig. 3A). The protein expression level clearly increased when the BOCK concentration exceeded 0.1 mM and the incubation time exceeded 4 h (Fig. 3B). The flow cytometry results also revealed that the BiCAR could be efficiently induced by BOCK addition in a concentration dependent manner (Fig. S2D-S2F). In addition, the periodic addition and withdrawal of BOCK demonstrated that the system possessed extremely high efficiency and flexible reversibility (Fig. 3C). To confirm that the regulation of the BOCK-induced CAR protein is focused on the translation process, we determined the transcript level of the CAR protein (Fig. 3D). The qRT-PCR assay demonstrated that the CAR mRNA levels were similar between conventional CAR-T cells and BiCAR-T cells, regardless of the presence or absence of BOCK. This finding confirmed that the BOCK induced genetic code expansion system is regulated at the translation level. Compared with other switches functioning in the transcriptional process, the response of the BiCAR system was quicker.

Moreover, we detected the levels of three general readouts related to CAR-T cell function, TNF-α, CD107a, and GZMB. Flow cytometry showed that the presence of BOCK increased the extent of CAR-T cell activation induced by antigen stimulation (Fig. 3E). Next, we tested the cytotoxicity of BiCAR system in primary T cells. The results of coculture with tumor cells showed that the cytotoxicity of BiCAR-T cells was tunable based on the BOCK dose, and was slightly lower than that of conventional CAR-T cells at concentrations up to 5 mM (Fig. 3F).

The level of CRS induced by vigorous activation is a significant indicator of CAR-T safety. Next, we assessed the CRS level in BiCAR system when faced with tumor cells, including GM-CSF, IFN-γ, IL-2, and TNF-α. To inhibit cytokine release, the BiCAR system was closed through BOCK withdrawal. Dasatinib was introduced as a positive control to prevent CAR-T cell activation [26]. Flow cytometry was used to measure the cytokine levels. The

results demonstrated that the BiCAR system efficiently inhibited cytokines release, similar to the effects induced by dasatinib (Fig. S3A), indicating the greater safety of the BiCAR-T system than the conventional CAR-T system. We also found that BiCAR-T cells exhibited strong cytotoxicity against B-ALL patient-derived $CD19^+$ tumor cells (Fig. S3B). Collectively, our data demonstrated that the reversible BOCK-induced switch can control the CAR-T cells activation and inactivation to achieve flexible anti-tumor effects in vitro.

The BiCAR system potentially influences the differentiation and persistence of CAR-T cells by inhibiting CAR-tonic signaling

CAR-T cell therapy has undoubtedly become a highly efficacious strategy for patients, especially those with B-cell malignancies. However, CAR protein expression can induce continuous and excessive T cell activation without ligands, exogeneous cytokines, or feeder cell stimulation, which is called CAR-tonic signaling [47]. In the absence of ligands, constitutive tonic signaling forces CAR-T cells differentiation into effectors and upregulates the levels of immune checkpoint proteins (PD-1, LAG-3, and CTLA-4) [20, 47]. This process has been increasingly recognized as a cause of poor anti-tumor efficacy, impaired survival, and reduced persistence in vivo. Therefore, exploring and optimizing the CAR-tonic signaling has been a significant topic for CAR-T therapy. During the production of BiCAR-T cells, we unexpectedly found that the BOCK induced BiCAR system could partly decrease CAR-tonic signaling.

After primary $CD3^+$ T cell separation, we manufactured BiCAR-T cells under two different conditions, with and without BOCK (Fig. 4A). Western blot results showed that persistent BOCK addition partly increased the phosphorylation levels of CAR downstream signals, including LCK, ZAP70, LAT, SLP76, and PLCγ1, even without antigen stimulation compared to that in the group lacking BOCK (Fig. 4B and S2G). Moreover, CD69 and CD25 were mildly activated by the addition of BOCK, similar to their effects on conventional CAR-T cells (Fig. 4C). These findings suggested that the BiCAR system can decrease the tonic signaling in the absent of BOCK. We also found that the levels of negative immune regulatory factors (PD-1 and CTLA-4) in BiCAR-T cells were lower than those in BiCAR-T cells with BOCK addition or conventional CAR-T cells (Fig. 4D and E). The T cell subset and differentiation status are considered significant factors for long persistence and CAR-T therapy efficacy [13]. Interestingly, our results indicated that the BiCAR system influences the differentiation during the in vitro culture period. The BiCAR group without BOCK addition presented the greatest ratio of T_{CM} and T_N, which suggested the superior persistence of CAR-T cells in vivo (Fig. 4F). These results demonstrated that the BiCAR system can partly inhibit the tonic signaling when BOCK was absent during the CAR-T cell preparation stage in vitro, which has the potential to improve CAR-T cell persistence and final efficiency.

BOCK controls anti-tumor effects mediated by the BiCAR system in mice

To verify the biosafety of BOCK in vivo, we first evaluated the long-term BOCK uptake in mice via intraperitoneal injection. Thirty days of BOCK administration did not result in any weight abnormalities (Fig. 5A). In addition, routine blood examination did not reveal any abnormal anomaly indices (Fig. S3C). These findings indicated that BOCK has the potential as a therapeutic agent in vivo without obvious toxic side-effects. Next, we evaluated the efficacy of CAR protein expression mediated by the BiCAR system and BOCK in vivo. BiCAR-T cells were injected intraperitoneally into the mice, and BOCK was subsequently injected. After 24 h, the peritoneal free cells were collected for flow cytometric analysis. CAR protein expression was initiated after BOCK injection and an inducer-dose-dependent increase was observed in vivo (Fig. 5B).

Furthermore, to evaluate the anti-tumor efficacy of BiCAR system in vivo, we established a xenograft leukemia model in NOG mice (Fig. 5C). Nalm6-Luc cells were intravenously engrafted into mice. After 7 days, the mice were randomly assigned to four groups and individually received conventional CAR-T cells, BiCAR-T cells without BOCK, or BiCAR-T cells with BOCK intraperitoneally injected at 20 mg per mouse every two days. To monitor tumor burden progression and assess anti-tumor activity in different groups, we evaluated tumor growth in each group by measuring luciferase-catalyzed bioluminescence every 7 days (Fig. 5D −5 F). We found that in the conventional CAR-T cells group, tumor cells were eliminated on approximately Day14, indicating a significant and expected anti-tumor efficacy. In the two groups of BiCAR-T cells, the anti-tumor efficacy was strongly dependent on BOCK. Compared with that in the control group, the tumor burden in the absence of BOCK significantly increased without obvious suppression. However, in the group treated with BOCK, the tumor burden was significantly inhibited and was similar to or slightly lower than that in the conventional CAR-T cells group. Subsequently, we observed the prolonged survival in mice that received BiCAR-T cells and BOCK, compared to those in the BOCK free group (Fig. 5E). Collectively, these results demonstrated that the cytotoxic activity and anti-tumor effect of BiCAR-T cells could be flexibly controlled by BOCK in mice.

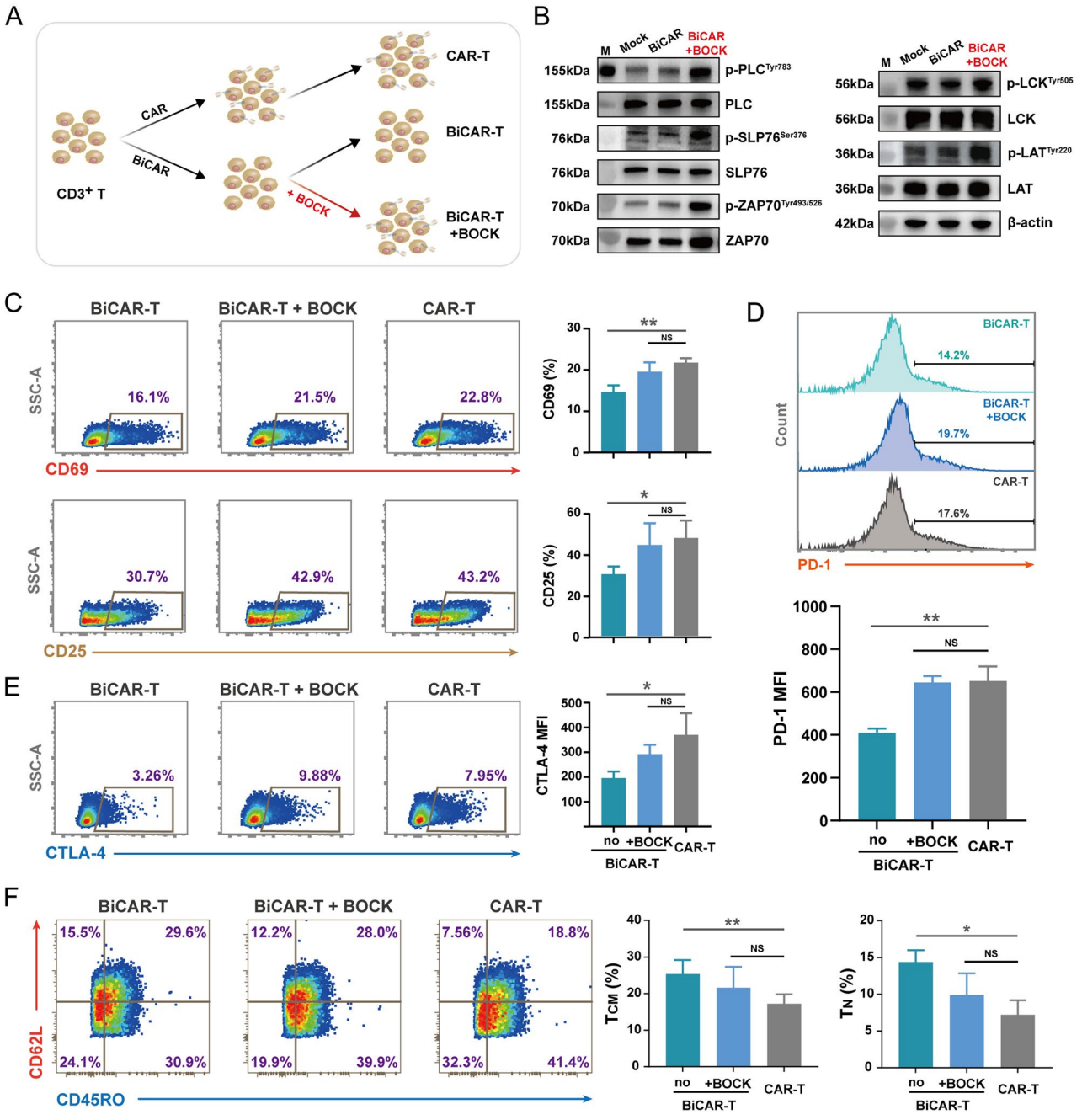

Fig. 4 Phenotypic differences between BiCAR-T cells and conventional CAR-T cells in terms of differentiation and persistence. **A** Schematic diagram showing the manufacturing and cultivation process of BiCAR-T cells in the absence or presence of BOCK. **B** Western blot assay showed that BOCK-induced CAR protein expression could increase the downstream phosphorylation events of CAR signaling without antigen stimulation. Without BOCK incubation, the phosphorylation levels were similar to those in the mock group. **C** Flow cytometry showed CD69 and CD25 protein expression in different groups. **D** Flow cytometry showed PD-1 expression in different groups. **E** Flow cytometry showed CTLA-4 expression in different groups. **F** Flow cytometry dot plots showed the expression of CD62L and CD45RO in different CAR-T cells, and the percentages of T_{CM} and T_N subsets were counted. The data are reported as the means ± SDs ($n = 3$). *$p < 0.05$, **$p < 0.01$, ***$p < 0.001$, not significant (ns) by t tests

Application of the BiCAR system in NK cell therapy

In addition to T cells, several other immune cells-based immunotherapies have been explored as new approaches and choices for clinical treatment. NK cells have been gradually applied in adoptive cell therapy. Compared to T cell therapy, NK cell has potential advantages, including fewer toxic side-effects without GvHD, more universal cytotoxicity without MHC restriction, and more rapid and convenient manufacturing processes with allogeneic sources [48, 49]. Similar to CAR-T therapy, CAR

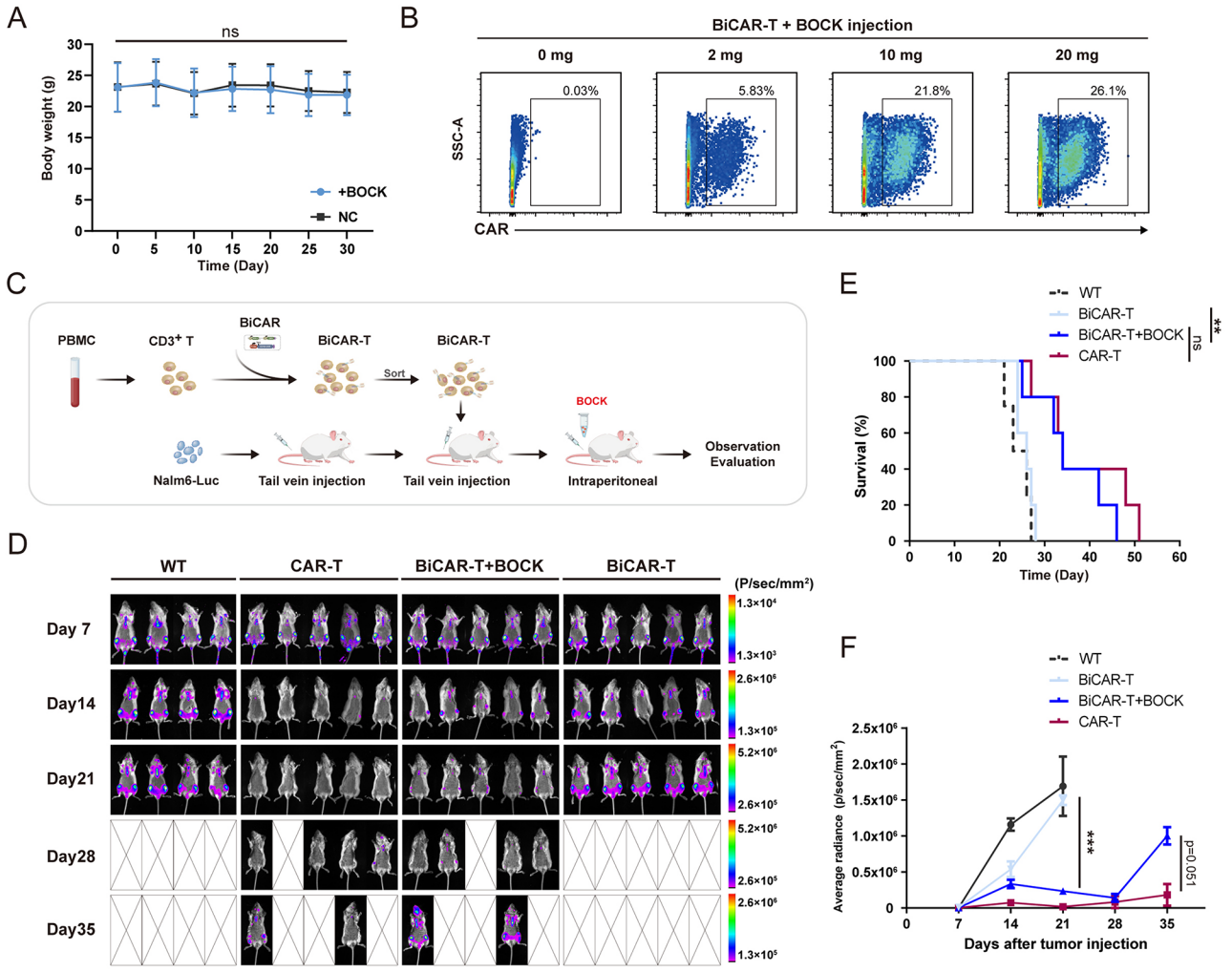

Fig. 5 Anti-tumor capability of BiCAR-T cells in mice. **A** Body weights of mice that were injected with BOCK every two days for one month. The data are reported as the means ± SDs ($n = 6$). **B** BiCAR-T cells were injected intraperitoneally, followed by BOCK injection. After 24 h, the peritoneal cells were collected and stained for CAR protein detection via flow cytometry. **C** The experimental design for assessing the anti-tumor efficacy of BOCK induced BiCAR system in xenograft leukemia mouse model. The pattern was created with BioGDP.com [58]. **D** Analysis of tumor burden progression in mice via bioluminescence imaging every 7 days. **E** The survival status of the mice in the different groups. **F** Quantification analyzation of the tumor burden by the average luminescence. *$p < 0.05$, **$p < 0.01$, ***$p < 0.001$, not significant (ns) by t or Mantel-Cox tests

protein loading significantly improves the anti-tumor efficacy of NK cells and a series of clinical tests about CAR-NK therapy for hematological malignancies and solid tumors have been performed [50, 51]. Therefore, we next assessed the use of the BiCAR system in NK cell therapy. We first constructed BiCAR-NK cells based on NK92 cells, a cell line that originated from NK cell and had been approved for clinical tests [52]. Without BOCK, the CAR protein could not be detected, while in the presence of BOCK, the CAR protein was translated in a dose dependent manner (Fig. 6A). Subsequently, the results of the coculture cytotoxicity assay demonstrated that BOCK-induced CAR-NK cells could kill cancer cells effectively, which was obviously superior to the cytotoxicity of the group without BOCK (Fig. 6B). Furthermore, flow cytometry showed that critical markers of NK cells were significantly increased with increasing BOCK concentration, including NKG2D, CD107a, CD69, and IFN-γ (Fig. 6C).

Furthermore, to evaluate the anti-tumor efficacy of BiCAR-NK in vivo, we established a xenograft leukemia model in NOG mice. Similar to that in BiCAR-T system, Nalm6-Luc cells were intravenously engrafted into mice. After 7 days, the mice were randomly assigned to four groups (five mice per group) and individually received conventional CAR-NK cells, BiCAR-NK cells without BOCK, or BiCAR-NK cells with BOCK addition. NK cell reinfusion was performed four times, respectively on Day8, Day15, Day22, and Day29. BOCK was intraperitoneally injected at a dose of 20 mg per mouse every two days. To monitor tumor burden progression and assess anti-tumor activity in different groups, we evaluated

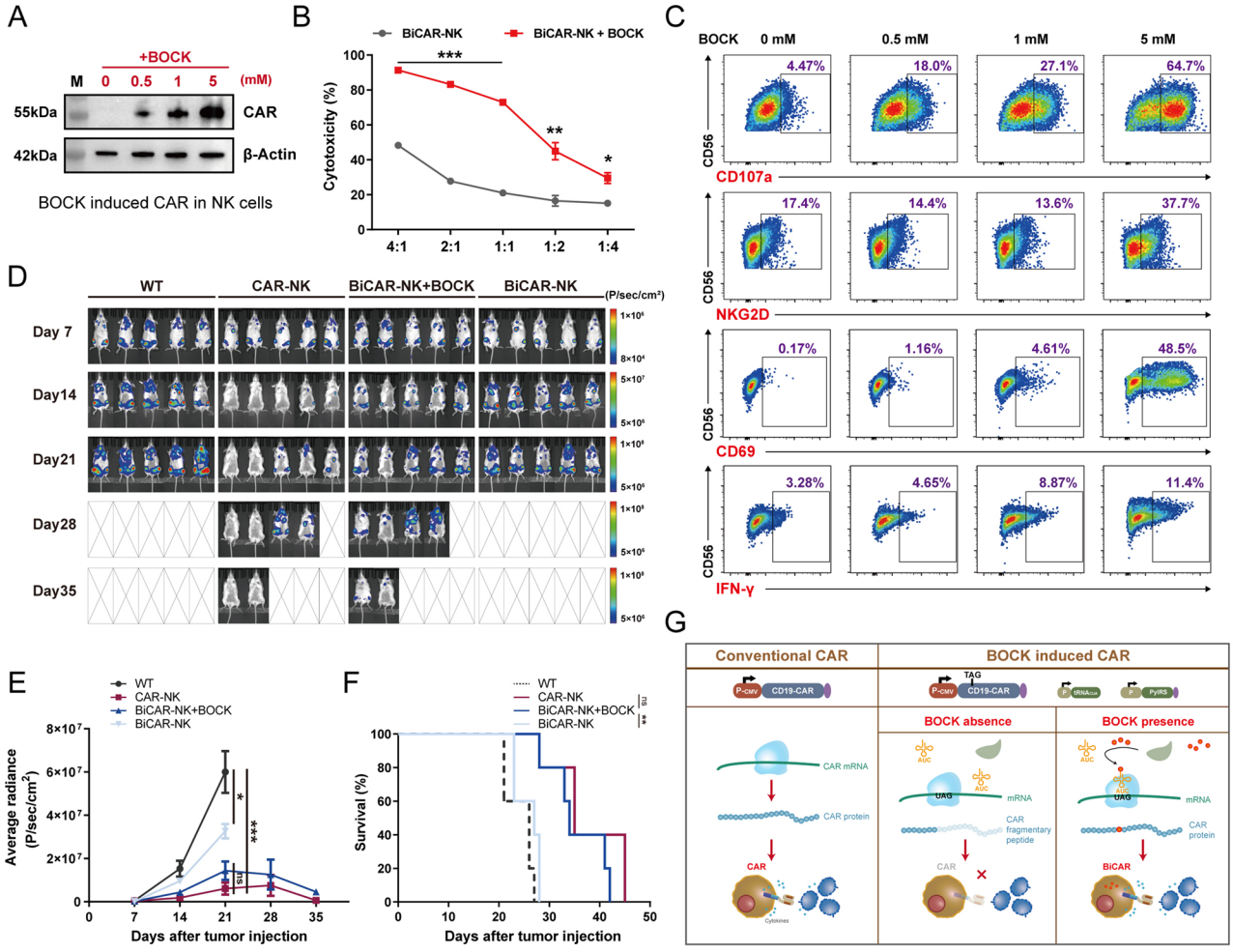

Fig. 6 Characterization and cytotoxicity of the BiCAR system in NK cells. **A** Western blot assay showed that the BOCK could induce BiCAR system in NK92 cells. **B** The cytotoxicity of BiCAR-NK cells cocultured with Nalm6-Luc cells and BOCK for 24 h at E/T ratios (4:1, 2:1, 1:1, 1:2, and 1:4). The data are reported as the means ± SDs ($n = 3$). **C** Flow cytometry analysis of CD107a degranulation, and NKG2D, CD69, and IFN-γ expression in BiCAR-NK cells with BOCK in different concentration when they were cocultured with Nalm6-Luc for 6 h. **D** Analysis of tumor burden progression in mice by bioluminescence imaging every 7 days ($n = 5$). **E** Quantification analyzation of tumor burden by the average luminescence. **F** The survival status of mice in the different groups. **G** Schematic showing the BiCAR device design and mechanism. *$p < 0.05$, **$p < 0.01$, ***$p < 0.001$, not significant (ns) by t or Mantel-Cox tests

tumor growth in each group by measuring luciferase-catalyzed bioluminescence every 7 days (Fig. 6D and E). We found that in the conventional CAR-NK group, tumor cells were eliminated on Day14, indicating a significant and expected anti-tumor efficacy. In the two groups of BiCAR-NK cells, the anti-tumor efficacy was strongly dependent on BOCK. In the absence of BOCK, the tumor burden significantly increased, although it was slightly lower than that in the control group. However, in the group treated with BOCK, the tumor burden was significantly inhibited and was similar to or slightly lower than that in the conventional CAR-NK cells group. Subsequently, we observed the prolonged survival in mice that received BiCAR-NK cells and BOCK, compared to that in the BOCK free group (Fig. 6F). Collectively, these results demonstrated that the cytotoxic activity and anti-tumor effect of BiCAR-NK cells could be flexibly controlled by BOCK in mice. These results revealed that the BiCAR system has the potential to function in various immune cell-dependent therapies.

Discussion

In recent years, CAR-T cell therapy has achieved tremendous success in the clinical treatment of B-cell malignancies. However, the notable anti-tumor effects have been partly offset by a series of unpredictable and uncontrollable side-effects, such as CRS, ICANS, and high recurrence rates, which could be fatal in patients. Synthetic and genetic biology have provided new avenues for solving these problems, including a series of logic-gated and switch-receptor strategies [23]. However, major approaches have still been applied in the laboratory, but

few have been demonstrated clinically to improve the efficacy or decrease the side-toxicity for CAR-T therapy, thereby suggesting the need for further optimization and exploration [53].

Here, we developed a reversible switch for CAR-T cells via a genetic code expansion system to flexibly and effectively control CAR expression and its anti-tumor effect both in vitro and in vivo. The termination codon TAG was inserted into the cassette of the CAR protein, which resulted in early termination of CAR protein translation and closed the anti-tumor capacity. When the unnatural amino acid BOCK is present, it can combine with the orthogonal tRNA/aaRS pairs. Then, the complex recognizes the termination codon and translates the whole CAR protein, enabling its anti-tumor function. We first demonstrated that BOCK could freely control the expression of CAR protein (Fig. 1). Our results showed that BOCK could regulate CAR signaling transduction, the activation state, cytokine secretion, and cytotoxicity in T cells (Figs. 2 and 3). The system showed sensitive reversibility, in which BOCK withdrawal quickly induced the degradation of CAR protein and closed CAR-T function. Moreover, we unexpectedly found that the BiCAR system could inhibit the tonic signaling when the BOCK was absent during the CAR-T cell preparation stage in vitro which altered the state of differentiation. These findings indicated the potential to improve CAR-T cells persistence and final efficiency (Fig. 4). The experiments in leukemia model in NOG mice verified that BOCK could control the tumor killing ability of CAR-T cells (Fig. 5). Finally, we also transplanted this device into NK cells, to demonstrate the universality of BOCK-induced CAR therapy in different types of immune cells (Fig. 6). The BOCK-controlled reversible switch established a proof of concept for immunotherapy strategies on the basis of the genetic code expansion system, not only in T cells, but also in other immune cells. Compared with several recent studies reporting small-molecular-controlled gene circuits [25–29, 32, 33], the BiCAR system has several advantages: (1) The insertion of the TAG stop codon could completely close CAR protein expression in the absence of BOCK, without any leaky activity. (2) The regulation of the BOCK-induced CAR protein is focused on the translation process and BOCK addition could quickly induce CAR protein translation. (3) BOCK withdrawal could quickly induce the degradation of CAR protein and closed CAR-T function, indicating sensitivity and absolute reversibility.

Despite the flexible and efficient regulatory effects of the BOCK-induced CAR system both in vivo and in vitro, several limitations need further optimization and improvement for clinical application. The random and unintended incorporation of BOCK in other termination codons might disturb T cells function. Additionally, the dosage of unnatural amino acids should be further tested and observed, although numerous noncanonical amino acids have been used as food additives and nutritional supplements [54]. During the manuscript preparation, a quadruplet codon translation system was designed and applied for the biosynthesis of peptides encoding UAAs in living cells. This system can be efficiently used to remold existing proteins and does not disturb the internal proteins with a TAG stop codon [55]. Moreover, our in vitro and in vivo assays revealed that the cytotoxicity of BiCAR system was slightly lower than that of the conventional CAR system, although the BiCAR cells had been sorted via flow cytometry. We hypothesized that the difference in cytotoxicity was due to the suboptimal translational efficacy and UAA utilization [56, 57]. It is necessary to improve the translation efficacy of the BiCAR system for further application. In conclusion, we established a reversible CAR device that enables flexible control of CAR activity. The system provides a potential for more effective, secure, and clinically available CAR-based cellular immunotherapies (Fig. 6G).

Conclusions

In this study, we designed and engineered a controllable and reversible switch for CAR-T therapy via a genetic code expansion system, which notably improved the safety and controllability of CAR-based cellular immunotherapies.

Abbreviations

CAR-T	Chimeric antigen receptor T
B-ALL	B acute lymphoblastic leukemia
CRS	Cytokine release syndrome
ICANS	Immune effector cell-associated neurotoxicity syndrome
aaRS	Aminoacyl-tRNA synthetase
UAA	Unnatural amino acid
PylRS	Pyrrolysyl-aaRS
BOCK	N-ε-((tert-butoxy) carbonyl)-l-lysine
PBMCs	Peripheral blood mononuclear cells
NOG mice	NOD.Cg-Prkdcscid mice
HEK293T	Human embryonic kidney 293T
BiCAR	BOCK induced CAR
F-BiCAR	The front BiCAR
M-BiCAR	The middle BiCAR
R-BiCAR	The rear BiCAR
JT	Jurkat T

Supplementary Information

The online version contains supplementary material available at https://doi.org/10.1186/s13045-024-01648-0.

Supplementary Material 1

Supplementary Material 2

Acknowledgements

Not applicable.

Author contributions
Y.L., L.A., and X.W. designed the project, wrote the manuscript, and generated figures. X.Z., Q.W., and C.Z. designed and supervised the studies and reviewed the manuscript. Y.L.L.A. and Y.D. conducted experiments, analyzed results. All authors read and approved the final manuscript.

Funding
This work was supported by the National Natural Science Foundation of China (No. 82300256 and 82341201), the Natural Science Foundation of Chongqing, China (No. CSTB2022NSCQ-MSX1287), the Science and Technology Project of Chongqing Municipal Education Commission (KJQN202312804), the Young Doctor Talent Incubation Program of Xinqiao Hospital (No. 2022YQB016), the Discipline Talent Development Special Project of Second Affiliated Hospital, Army Medical University (2022XKRC001), and the Discipline Capacity Enhancement Project of Second Affiliated Hospital, Army Medical University.

Data availability
The data that support the findings of this study are available from the corresponding author upon reasonable request.

Declarations

Ethics approval and consent to participate
The samples from healthy donors and patients were approved and obtained by the Institutional Review Board at Xinqiao Hospital, Army Medical University (2024-067-01). All the animal studies were approved by the Army Medical University Institutional Animal Care and Use Committee (AMUWEC20234644).

Consent for publication
Not applicable.

Competing interests
The authors declare no competing interests.

Author details
[1]Medical Center of Hematology, Xinqiao Hospital of Army Medical University, Chongqing 400037, China
[2]State Key Laboratory of Trauma and Chemical Poisoning, Chongqing Key Laboratory of Hematology and Microenvironment, Chongqing 400037, China
[3]Jinfeng Laboratory, Chongqing 401329, China

Received: 9 October 2024 / Accepted: 2 December 2024
Published online: 18 December 2024

References

1. June CH, O'Connor RS, Kawalekar OU, Ghassemi S, Milone MC. CAR T cell immunotherapy for human cancer. Science. 2018;359(6382):1361–5.
2. Wei J, Guo Y, Wang Y, Wu Z, Bo J, Zhang B, et al. Clinical development of CAR T cell therapy in China: 2020 update. Cell Mol Immunol. 2021;18(4):792–804.
3. Labanieh L, Mackall CL. CAR immune cells: design principles, resistance and the next generation. Nature. 2023;614(7949):635–48.
4. Luo Y, Gao L, Liu J, Yang L, Wang L, Lai X, et al. Donor-derived Anti-CD19 CAR T cells GC007g for relapsed or refractory B-cell acute lymphoblastic leukemia after allogeneic HSCT: a phase 1 trial. EClinicalMedicine. 2024;67:102377.
5. Sun W, Liang A-B, Huang H, Huang X-J. Strategies to optimize chimeric antigen receptor T-cell therapy in hematologic malignancies: Chinese experience. Haematologica. 2023;108(8):2011–28.
6. Mullard A. FDA approves fourth CAR-T cell therapy. Nat Rev Drug Discov. 2021;20(3):166.
7. Hu Y, Feng J, Gu T, Wang L, Wang Y, Zhou L, et al. CAR T-cell therapies in China: rapid evolution and a bright future. Lancet Haematol. 2022;9(12):e930–41.
8. Chavez JC, Bachmeier C, Kharfan-Dabaja MA. CAR T-cell therapy for B-cell lymphomas: clinical trial results of available products. Ther Adv Hematol. 2019;10:2040620719841581.
9. Mei H, Hari P, Hu Y. Exercise CALM and make CAR-T therapy work better. Sci Bull (Beijing). 2022;67(19):1925–8.
10. Fajgenbaum DC, June CH. Cytokine storm. N Engl J Med. 2020;383(23):2255–73.
11. Gust J, Hay KA, Hanafi L-A, Li D, Myerson D, Gonzalez-Cuyar LF, et al. Endothelial activation and blood-brain barrier disruption in neurotoxicity after adoptive immunotherapy with CD19 CAR-T cells. Cancer Discov. 2017;7(12):1404–19.
12. Huang Y, Si X, Shao M, Teng X, Xiao G, Huang H. Rewiring mitochondrial metabolism to counteract exhaustion of CAR-T cells. J Hematol Oncol. 2022;15(1):38.
13. Liu Y, An L, Huang R, Xiong J, Yang H, Wang X, et al. Strategies to enhance CAR-T persistence. Biomark Res. 2022;10(1):86.
14. Bulliard Y, Andersson BS, Baysal MA, Damiano J, Tsimberidou AM. Reprogramming T cell differentiation and exhaustion in CAR-T cell therapy. J Hematol Oncol. 2023;16(1):108.
15. Lai P, Chen X, Wang Y, Wang J, Zhang Y, Geng S, et al. C3aR costimulation enhances the antitumor efficacy of CAR-T cell therapy through Th17 expansion and memory T cell induction. J Hematol Oncol. 2022;15(1):68.
16. Mazinani M, Rahbarizadeh F. CAR-T cell potency: from structural elements to vector backbone components. Biomark Res. 2022;10(1):70.
17. Shimabukuro-Vornhagen A, Böll B, Schellongowski P, Valade S, Metaxa V, Azoulay E, et al. Critical care management of chimeric antigen receptor T-cell therapy recipients. CA Cancer J Clin. 2022;72(1):78–93.
18. Westin JR, Oluwole OO, Kersten MJ, Miklos DB, Perales M-A, Ghobadi A, et al. Survival with Axicabtagene Ciloleucel in large B-Cell lymphoma. N Engl J Med. 2023;389(2):148–57.
19. Locke FL, Miklos DB, Jacobson CA, Perales M-A, Kersten M-J, Oluwole OO, et al. Axicabtagene Ciloleucel as Second-Line therapy for large B-Cell lymphoma. N Engl J Med. 2022;386(7):640–54.
20. Ajina A, Maher J. Strategies to address chimeric Antigen receptor Tonic Signaling. Mol Cancer Ther. 2018;17(9):1795–815.
21. Long AH, Haso WM, Shern JF, Wanhainen KM, Murgai M, Ingaramo M, et al. 4-1BB costimulation ameliorates T cell exhaustion induced by tonic signaling of chimeric antigen receptors. Nat Med. 2015;21(6):581–90.
22. Chen J, Qiu S, Li W, Wang K, Zhang Y, Yang H, et al. Tuning charge density of chimeric antigen receptor optimizes tonic signaling and CAR-T cell fitness. Cell Res. 2023;33(5):341–54.
23. Teng F, Cui T, Zhou L, Gao Q, Zhou Q, Li W. Programmable synthetic receptors: the next-generation of cell and gene therapies. Signal Transduct Target Ther. 2024;9(1):7.
24. Di Stasi A, Tey S-K, Dotti G, Fujita Y, Kennedy-Nasser A, Martinez C, et al. Inducible apoptosis as a safety switch for adoptive cell therapy. N Engl J Med. 2011;365(18):1673–83.
25. Diaconu I, Ballard B, Zhang M, Chen Y, West J, Dotti G, et al. Inducible Caspase-9 selectively modulates the toxicities of CD19-Specific chimeric Antigen receptor-modified T cells. Mol Ther. 2017;25(3):580–92.
26. Mestermann K, Giavridis T, Weber J, Rydzek J, Frenz S, Nerreter T et al. The tyrosine kinase inhibitor dasatinib acts as a pharmacologic on/off switch for CAR T cells. Sci Transl Med. 2019; 11(499).
27. Cao W, Geng ZZ, Wang N, Pan Q, Guo S, Xu S, et al. A reversible Chemogenetic switch for Chimeric Antigen Receptor T Cells. Angew Chem Int Ed Engl. 2022;61(10):e202109550.
28. Wu Y, Liu Y, Huang Z, Wang X, Jin Z, Li J, et al. Control of the activity of CAR-T cells within tumours via focused ultrasound. Nat Biomed Eng. 2021;5(11):1336–47.
29. Smole A, Benton A, Poussin MA, Eiva MA, Mezzanotte C, Camisa B et al. Expression of inducible factors reprograms CAR-T cells for enhanced function and safety. Cancer Cell. 2022; 40(12).
30. Huang Z, Wu Y, Allen ME, Pan Y, Kyriakakis P, Lu S, et al. Engineering light-controllable CAR T cells for cancer immunotherapy. Sci Adv. 2020;6(8):eaay9209.
31. Li H-S, Wong NM, Tague E, Ngo JT, Khalil AS, Wong WW. High-performance multiplex drug-gated CAR circuits. Cancer Cell. 2022; 40(11).
32. Qi J, Tsuji K, Hymel D, Burke TR, Hudecek M, Rader C, et al. Chemically programmable and switchable CAR-T therapy. Angew Chem Int Ed Engl. 2020;59(29):12178–85.
33. Yang L, Yin J, Wu J, Qiao L, Zhao EM, Cai F et al. Engineering genetic devices for in vivo control of therapeutic T cell activity triggered by the dietary molecule resveratrol. Proc Natl Acad Sci U S A. 2021; 118(34).
34. Labanieh L, Majzner RG, Klysz D, Sotillo E, Fisher CJ, Vilches-Moure JG et al. Enhanced safety and efficacy of protease-regulated CAR-T cell receptors. Cell. 2022; 185(10).
35. Ling J, O'Donoghue P, Söll D. Genetic code flexibility in microorganisms: novel mechanisms and impact on physiology. Nat Rev Microbiol. 2015;13(11):707–21.

36. Buckingham RH, Kurland CG. Codon specificity of UGA suppressor tRNATrp from Escherichia coli. Proc Natl Acad Sci U S A. 1977;74(12):5496–8.
37. Köhrer C, Sullivan EL, RajBhandary UL. Complete set of orthogonal 21st aminoacyl-tRNA synthetase-amber, ochre and opal suppressor tRNA pairs: concomitant suppression of three different termination codons in an mRNA in mammalian cells. Nucleic Acids Res. 2004;32(21):6200–11.
38. Chin JW. Expanding and reprogramming the genetic code of cells and animals. Annu Rev Biochem. 2014;83:379–408.
39. Davis L, Chin JW. Designer proteins: applications of genetic code expansion in cell biology. Nat Rev Mol Cell Biol. 2012;13(3):168–82.
40. Shi N, Yang Q, Zhang H, Lu J, Lin H, Yang X, et al. Restoration of dystrophin expression in mice by suppressing a nonsense mutation through the incorporation of unnatural amino acids. Nat Biomed Eng. 2022;6(2):195–206.
41. Chen C, Yu G, Huang Y, Cheng W, Li Y, Sun Y, et al. Genetic-code-expanded cell-based therapy for treating diabetes in mice. Nat Chem Biol. 2022;18(1):47–55.
42. Ma S, Zhang J, Lu W, Liu Y, Xia Q. SAA-Cas9: a tunable genome editing system with increased bio-safety and reduced off-target effects. J Genet Genomics. 2019;46(3):145–8.
43. Lee KJ, Kang D, Park H-S. Site-specific labeling of proteins using unnatural amino acids. Mol Cells. 2019;42(5):386–96.
44. Mills EM, Barlow VL, Jones AT, Tsai Y-H. Development of mammalian cell logic gates controlled by unnatural amino acids. Cell Rep Methods. 2021;1(6):100073.
45. van Husen LS, Katsori A-M, Meineke B, Tjernberg LO, Schedin-Weiss S, Elsässer SJ. Engineered Human Induced Pluripotent cells enable genetic code expansion in Brain Organoids. ChemBioChem. 2021;22(22):3208–13.
46. Prasad V, Immunotherapy. Tisagenlecleucel - the first approved CAR-T-cell therapy: implications for payers and policy makers. Nat Rev Clin Oncol. 2018;15(1):11–2.
47. Frigault MJ, Lee J, Basil MC, Carpenito C, Motohashi S, Scholler J, et al. Identification of chimeric antigen receptors that mediate constitutive or inducible proliferation of T cells. Cancer Immunol Res. 2015;3(4):356–67.
48. Shang J, Hu S, Wang X. Targeting natural killer cells: from basic biology to clinical application in hematologic malignancies. Exp Hematol Oncol. 2024;13(1):21.
49. Dagher OK, Posey AD. Forks in the road for CAR T and CAR NK cell cancer therapies. Nat Immunol. 2023;24(12):1994–2007.
50. Huang R, Wen Q, Zhang X. CAR-NK cell therapy for hematological malignancies: recent updates from ASH 2022. J Hematol Oncol. 2023;16(1):35.
51. Van den Eynde A, Gehrcken L, Verhezen T, Lau HW, Hermans C, Lambrechts H, et al. IL-15-secreting CAR natural killer cells directed toward the pan-cancer target CD70 eliminate both cancer cells and cancer-associated fibroblasts. J Hematol Oncol. 2024;17(1):8.
52. Klingemann H. The NK-92 cell line-30 years later: its impact on natural killer cell research and treatment of cancer. Cytotherapy. 2023;25(5):451–7.
53. Del Bufalo F, De Angelis B, Caruana I, Del Baldo G, De Ioris MA, Serra A, et al. GD2-CART01 for relapsed or Refractory High-Risk Neuroblastoma. N Engl J Med. 2023;388(14):1284–95.
54. Wu G. Important roles of dietary taurine, creatine, carnosine, anserine and 4-hydroxyproline in human nutrition and health. Amino Acids. 2020;52(3):329–60.
55. Costello A, Peterson AA, Lanster DL, Li Z, Carver GD, Badran AH. Efficient genetic code expansion without host genome modifications. Nat Biotechnol. 2024; Sep 11. https://doi.org/10.1038/s41587-024-02385-y
56. Ding W, Yu W, Chen Y, Lao L, Fang Y, Fang C, et al. Rare codon recoding for efficient noncanonical amino acid incorporation in mammalian cells. Science. 2024;384(6700):1134–42.
57. Shi Y, Shi N, Yang Y, Zheng Z, Xia Q. Unnatural amino acid-based ionic liquid enables oral treatment of nonsense mutation disease in mice. Adv Sci (Weinh). 2024;11(13):e2306792.
58. Jiang S, Li H, Zhang L, Mu W, Zhang Y, Chen T et al. Generic diagramming platform (GDP): a comprehensive database of high-quality biomedical graphics. Nucleic Acids Res 2024; Oct 29:gkae973.

Publisher's note